Hybrid Hydrocarbon/Fluorocarbon Nanoparticle Coatings for Environmentally Friendly Omniphobic Surfaces

*Donald Hill,[1] Henry Apsey [1] Andrew. R. Barron[1,2,3,4] and Shirin Alexander[1]**

[1]Energy Safety Research Institute (ESRI), Swansea University Bay Campus, Fabian Way, Swansea SA1 8EN, United Kingdom

[2]Arizona Institutes for Resilience (AIR), University of Arizona, Tucson, Arizona 85721, USA.

[3]Department of Chemistry and Department of Materials Science and Nanoengineering, Rice University, Houston, Texas 77005, USA.

[4]Faculty of Engineering, Universiti Teknologi Brunei, BE1410

Brunei Darussalam.

KEYWORDS: omniphobic, nanoparticles, carboxylic acid, green, fluorocarbon, environmentally-friendly.

*S.Alexander@swansea.ac.uk

ABSTRACT

The release of fluorocarbons (FCs) into the environment is a growing problem for the chemical industry. Fluorocarbons have been observed in increasing amounts across a range of different locations worldwide on account of environmental release of polymers, consumer products and a range of other sources. These compounds show long biological half-lives and have been linked to a number of negative toxicological effects. As such, their use should be restricted and eliminated where possible. In this paper, we have shown that the amount of fluorocarbon in omniphobic coatings formed from carboxylate-functionalized nanoparticles can be reduced by as much as 70% without compromising properties such as contact angle hysteresis (CAH) or sliding angle (SA). This reduction is made possible using approaches involving adsorbing hybrid hydrocarbon and fluorocarbon carboxylates chains onto commercially available aluminum oxide nanoparticles. The carboxylates are either co-adsorbed onto the same particles, referred to as chemically mixed (CM), or attached to different particles, which we have referred to as physically mixed (PM). Both of these types of surface show enhanced omniphobicity compared to coatings that had been functionalized by the same amount of the fluorinated carboxylate but did not contain any carboxylates bearing hydrocarbon chains. In addition, the sliding properties of synthetic faeces on these surfaces were tested in order to investigate the potential applications of this methodology. Similarly, it was observed that the amount of fluorocarbon in the coatings could be substantially reduced without significantly increasing the sliding angle of the mixture on the surface.

INTRODUCTION

It is well understood that adsorption of fluorocarbons onto surfaces is necessary to make them repellent towards water and oil.[1-4] The origin of this behavior is ascribed to the low surface energy of the CF_3 group, which reduces the wettability of oils and other low surface tension liquids on materials functionalized by fluorocarbons.[1-4] The high electronegativity of the F atoms reduces the ability of these compounds to interact via dispersive interactions, whilst the low polarizability of the C-F bonds limits the potential for hydrogen bonding interactions.[5-7] Although coatings functionalized by compounds possessing hydrocarbon moieties can be highly repellent to water, they are usually oleophilic. This is because the surface energy of the exposed hydrocarbon chains is too high to stop oils and other low surface tension liquids from spreading.[1-7] Because of this, fluorinated materials have been used with widespread success to create highly omni- and super-omniphobic surfaces in recent years. In addition to the low surface energy provided by the fluorinated groups, these coatings also possess suitable topographies to generate their low wettability.[1-7] Utilizing nanoparticles to create surface roughness has been frequently used in reports studying low wettability coatings as a result of their commercial availability and reactivity towards compounds that can lower their surface energy[1-4]. Silica nanoparticles have been heavily used to create omni and super-omniphobic coatings following reactions between the particles and fluorinated and perfluorinated silanes.[8-10] Similarly, metal oxide nanoparticles have been used as precursors for coatings that can repel organic liquids after functionalization with perfluorinated carboxylic acids.[11] More recently it has been shown that fluorinated coatings with smoother topographies are also capable of displaying substantial repellency towards water and organic liquids. Ma *et al* observed that it was possible to create surfaces with robust antifouling properties through dip coating glass samples in silica sols which also contained perfluoropolyether

triethoxysilane.[12] Their coatings were observed to show excellent stain resistance against artificial sweat and were highly resistant to mechanical wear.[12]

Despite their utility, a number of considerations exist surrounding the use of fluorocarbons in low surface energy coatings and functional materials. Fluorocarbons are not observed in nature and have been observed to bioaccumulate in food chains because of these compounds showing relatively long residence times inside animals following ingestion.[13] The *in-vivo* stability of fluorinated compounds is thought to be linked to the high energy required for enzymes to cleave the C-F covalent bonds, which results in them displaying long half lives in biological systems.[14] In addition, perfluorocarboxylates have been observed at variable concentrations in fresh and coastal waters throughout the world, which is especially worrying given that it is thought that large proportions of the fluorocarbons that are synthesized industrially are eventually released into the environment.[15] In addition to their negative environmental impact, fluorinated carboxylic acids such as perfluorooctanoic acid have been observed to cause a number of harmful toxicological effects in including cancers and liver abnormalities and have been shown to reduce antibody production.[16-18]

In light of their harmful toxicological effects and environmental concerns, it is prudent to study methods that employ lower amounts of fluorinated materials. In this paper, we have investigated two methods of reducing the fluorocarbon content in omniphobic coatings: the first method involves depositing coatings formed from aluminum oxide nanoparticles co-functionalized with both stearic and perfluorotetradecanoic acid, termed chemically mixed (CM) particles (Scheme 1). Whereas the second involves applying coatings containing different amounts of stearic and perfluorotetradecanoic acid functionalized aluminum oxide nanoparticles, which are referred to as physically mixed (PM) particles (Scheme 1). In this method, the carboxylates are not co-adsorbed

onto the same nanoparticles. The efficacy of these two types of coating for repelling both water and diiodomethane is compared and further evaluated against the nanoparticle coatings when they are solely functionalized with perfluorotetradecanoic acid. Previous work studying omniphobic coatings has focused on making the methodology greener through substituting long fluorinated chains with less environmentally harmful shorter chain analogues.[19, 20] Separately, it has also been studied that mixed hydrophilic/ fluorocarbon coatings formed from polyols and fluorinated alkanes can also act as non-stick coatings for nanoparticles on mineral surfaces.[21] It was observed that the fluorinated molecules disrupted the hydration layers present on mineral surfaces onto which hydroxyl groups of the polyols would otherwise adhere to.[21] However, to our knowledge, previous studies that examine the minimum threshold of fluorocarbon efficacy for creating coatings that are repellent to water and organic liquids have not yet been reported. In addition to this investigation, we have also studied the sliding behavior of viscoelastic solids on these surfaces, designed to simulate faecal material, in order to study the antifouling properties of these coatings. Although aluminum oxide nanoparticles have been shown to be harmful upon environmental release, these particles show lower DNA damage towards human lymphocytes than other types of nanoparticles.[22] Notably this includes SiO_2 nanoparticles, which have been widely used to prepare omniphobic coatings using similar methodologies.[1] Consequently, aluminum oxide nanoparticles have been selected for this investigation since studies show they may be less harmful towards humans if they were accidentally ingested.[22]

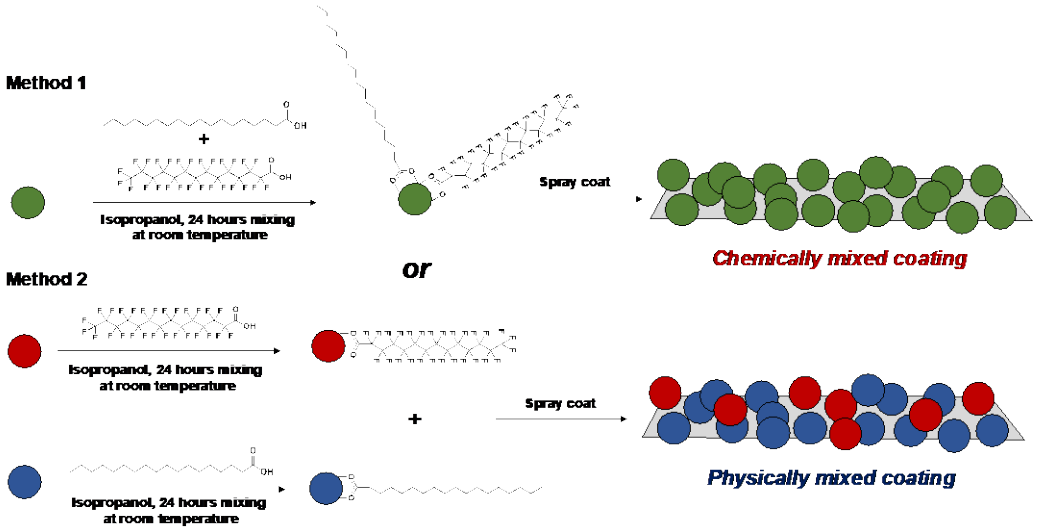

Scheme 1. Synthetic approaches undertaken to manufacture the chemically (Method 1) and physically (Method 2) mixed coatings.

RESULTS AND DISCUSSION

Surface adsorption of the carboxylic acids onto the nanoparticles. The loading of the carboxylic acids onto the nanoparticles was studied through TGA. Weight losses above 300 °C were attributed to the removal of chemically adsorbed carboxylates from the particles, in line with what we have observed in our previous studies.[11, 23-25] Grafting densities, were calculated using the method that we have discussed in our earlier publications.[11, 23, 24] It was observed that the grafting density of stearate onto the aluminum oxide was saturated when it reached a value of about 1.2 nm^{-2} (Table 1). Unsaturated surfaces were observed when the particles were immersed in solutions where the stearic acid concentration was below 5 mM. Adsorption of stearic acid onto the particles from a 1 mM solution was observed to create particles that showed a stearate grafting density of 0.6 nm^{-2} (Table 1). Whereas immersion of particles in a 3 mM solution generated particles that displayed a grafting density of 1.0 nm^{-2}. Using a 4 mM solution was observed to create particles that displayed a grafting density of 1.1 nm^{-2}.

The maximum grafting density of perfluorodecanoate on the surfaces was observed to be slightly higher and reached a plateau at about 1.7 nm^{-2} (Table 1). Similarly, the surface of the nanoparticles was observed to become almost fully saturated when the concentration of the FC carboxylic acid was between 2-5 mM. Immersion of the particles in a 2 mM perfluorotetradecanoic acid solution created particles that showed a grafting density of 1.1 nm^{-2}, whereas using a 3 mM solution was observed to generate a 1.5 nm^{-2} grafting density. Since this value was also observed when the particles were immersed in the 5 mM solution (Table 1) this indicates that the particles had become saturated with the fluorinated carboxylic acid. TGA heating profiles of the FC and HC functionalized particles are shown in the supporting information (SI, Figures S1a and b and Figures S2 and S3). Unfortunately, it was not possible to calculate the loadings of the individual FC and HC carboxylates when the particles had been immersed in solutions containing both of these carboxylic acids. Both carboxylates were observed to be removed at similar temperatures when TGA was performed on the CM particles.

Table 1. Carboxylate grafting densities observed for the particles following immersion in the carboxylic acid solutions[a].

Concentration of carboxylic acid/ mM	15	10	5	1
Perfluorodecanoate grafting density/ nm^{-2}	1.7	1.6	1.5	0.7
Stearate grafting density/ nm^{-2}	1.2	1.2	1.2	0.6

[a]Values are calculated from the TGA weight loss between 300-650 ºC using the method described in reference 23.

Chemical adsorption of the carboxylic acids onto the aluminum oxide was studied using infrared (IR) spectroscopy. IR analysis of the as received particulate showed a strong band below 1000 cm^{-1} due to the Al-O lattice vibrations and a wide band between 3200 and 3700 cm^{-1} ascribed to O-H stretching of the surface hydroxyl groups[11, 23, 24] (SI Figure S4a). Adsorption of perfluorotetradecanoic acid onto the particles was confirmed by the presence of intense C-F stretching bands between 1251 and 1156 cm^{-1} and a weaker C-O stretching band at 1667 cm^{-1}, confirming that the carboxylic acid had adsorbed as a carboxylate[11, 23, 26] (SI, Figure S4b). Bands ascribed to C-H stretching and CH_2 bending were observed between 2855 and 2961 cm^{-1} and 1467 cm^{-1} respectively in the IR spectra of the nanoparticles following immersion in the stearic acid solutions, indicating that the carboxylic acid had adsorbed onto the surface[11, 23, 24] (SI Figure 4c). Carboxylate asymmetric and symmetric stretches were observed at 1560 and 1411 cm^{-1} respectively, which showed that stearate was chemically adsorbed in the bridging coordination mode.[11, 26] Bands ascribed to C-F and C-H stretching were observed in the IR spectra of nanoparticles that had been immersed in solutions containing 5 mM stearic acid and 1 mM or lower perfluorooctanoic acid, in addition to carboxylate stretching bands. Residual O-H stretching bands were also observed in all of the IR spectra of the functionalized nanoparticles, indicating that some hydroxyl groups remained on the metal oxide following chemisorption of the carboxylic acids. The IR spectrum of the aluminum oxide nanoparticles after immersion in the solution containing 5 mM stearic acid and 1 mM perfluorotetradecanoic acid is displayed in Figure 1. In the mixed solutions it was observed that the fluorinated carboxylic acid would adsorb preferentially onto the particles over stearic acid. Consequently, the concentrations of perfluorotetradecanoic acid in the mixed solution were limited to 1 mM or below. As discussed, TGA shows that the particles are unsaturated using this concentration of the carboxylic acid. Consequently, this concentration range

allows the particles' surface to have an appreciable number of sites for stearic acid to adsorb onto. More detail about the competitive adsorption between the carboxylic acids is provided in the supporting information.

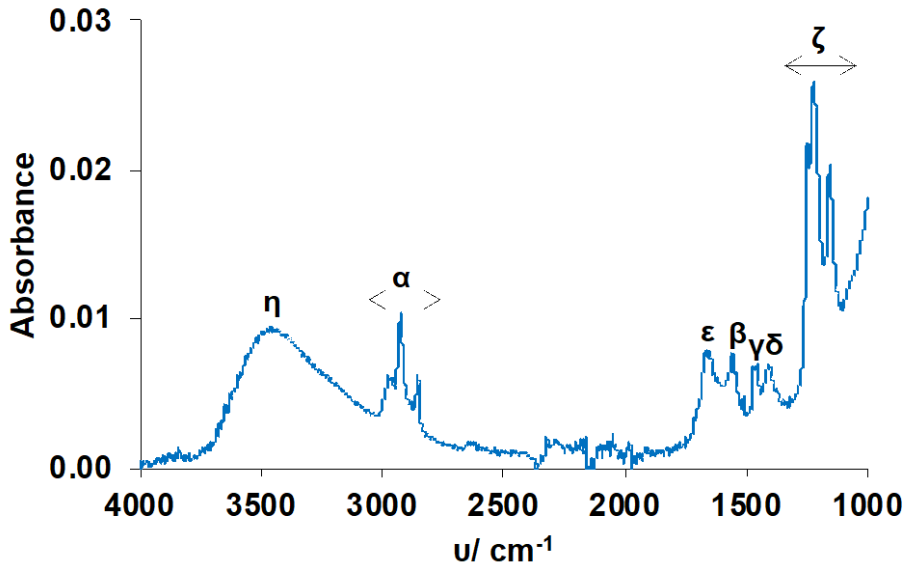

Figure 1. IR spectrum of the aluminum oxide nanoparticles (1000-4000 cm^{-1}) after immersion in the isopropanolic solution containing 1 mM perfluorotetradecanoic acid and 5 mM stearic acid. η = O-H stretch, α = C-H stretches, ε = carboxylate stretching band (perfluorodecanoate), β = carboxylate asymmetric stretching (stearate), γ = CH_2 scissoring, δ = carboxylate symmetric stretching (stearate), ζ = C-F stretching.

Investigations into coating morphology. SEM imaging performed on films created using the nanoparticles showed that they possessed rough morphologies formed from micro/ nanoscale features, similar to previous studies[11, 23, 24] (Figure 2 and SI Figures S7 to S11). Pores were observed inside and between the surface features, created because of the random packing of the nanoparticles inside the films. The porous nature of the coatings, formed as a result of the micro/ nanoscale roughness facilitates low wettability and low droplet adhesion since air becomes trapped

between the surface features, reducing the contact area between the droplet and the surface and thus increasing the contact angle.[2] Although the films possessed similar morphologies, it was observed using SEM that films that were completely saturated with perfluorotetradecanoate showed larger topographies than films formed from the hydrocarbon functionalized particles, or films deposited using the CM and PM nanoparticles (Figure 2 and SI Figures S7 to S11). This was confirmed using AFM where the fully fluorinated films showed significantly larger surface roughness, R_a, than the hydrocarbon functionalized films and also selected examples of the CM and PM coatings (Figure S12 and Table S1). It has been well studied that larger surface roughness leads enhanced liquid repellency.[2] Consequently, the lower wettability of the fluorinated films, which is discussed in detail in the wettability studies, could be the result of their greater surface roughness, in addition to the lower surface energy provided by the fluorinated groups.

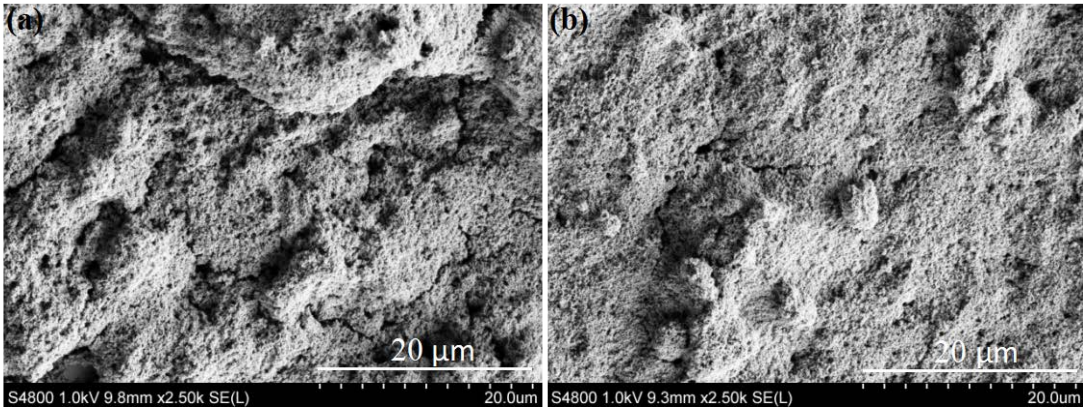

Figure 2. SEM images of the nanoparticle films, fully saturated with perfluorotetradecanoate (a) and fully saturated with stearate (b).

Wettability studies. The contact angles (CAs) and sliding angles (SAs) of water and diiodomethane on the nanoparticle coated surfaces were measured to study the omniphobic properties of the different coatings. It was observed that the coatings displayed water contact angles (WCAs) between 150-155º when they were immersed in 2 and 5 mM perfluoroteradecanoic

acid solutions (Figure 3a). The sliding angles of water droplets on nanoparticle coatings synthesized using the 5 mM perfluoroteradecanoic acid solution were observed to vary between 6-10°, whereas those observed for the coating prepared using the 2 mM perfluoroteradecanoic acid solution were slightly higher, between 18-21°. The high WCAs and low sliding angles are indicative of a Cassie-Baxter regime, where air is trapped between surface grooves and the water droplet only makes contact with the apex of surface features.[2] Reducing the concentration of perfluorotetradecanoate to 1 mM or below was observed to create less hydrophobic surfaces with WCAs reducing steadily from 148° to 56° (Figure 3a). Water droplets were observed to be strongly adherent onto these surfaces and would not roll off, even after tilting the samples to 90°. This indicates that large areas of the nanoparticles were not functionalized by carboxylates, which caused the surface to display Wenzel wetting, as opposed to Cassie-Baxter wetting.[2]

Diiodomethane CAs of nanoparticle coatings prepared using 2 and 5 mM perfluoroteradecanoic acid solutions were found to vary between 138-148° (Figure 3a). Reducing the concentration of perfluoroteradecanoic acid to 1 mM created surfaces that showed slightly lower CAs, ranging between 132-137 º. Below 1 mM, the diiodomethane contact angles were observed to reduce steadily until they reached values of 20-22 °, for 0.2 mM perfluoroteradecanoic acid solutions. By comparison to water droplets on these coatings, diiodomethane droplets were observed to roll off at much lower surface coverages of perfluoroteradecanoate. Diiodomethane sliding angles between 5-7 ° were observed for coatings prepared using 2 and 5 mM perfluoroteradecanoic acid solutions (Figure 3b). This behavior is ascribed to the lower surface tension and higher density of the liquid.[27, 28] Below 2 mM, larger inclinations were required to initiate diiodomethane droplet sliding on the surfaces. Coatings prepared from particles functionalized using 1 mM perfluoroteradecanoic acid solutions showed sliding angles between 17-21°, indicating that the

grafting density of perfluoroteradecanoic acid had dropped below a threshold where the liquid droplet was more adherent to the nanoparticles. In support this, the sliding angle of diiodomethane was observed to increase sharply upon lowering the concentration of the carboxylic acid further (Figure 3b) and diiodomethane droplets did not show sliding angles when the concentration of perfluoroteradecanoic acid was reduced below 0.6 mM.

Coatings prepared using nanoparticles that had been immersed in the mixed solutions showed different wetting behavior towards water and diiodomethane, relative to films prepared using solutions containing solely perfluorotetradecanoic acid. In these experiments the concentration of stearic acid was fixed at 5 mM and the concentration of perfluorotetradecanoic acid varied. As previously discussed, IR analysis indicated that perfluoroteradecanoic acid was adsorbed preferentially onto the nanoparticles over stearic acid. Consequently, the concentration of perfluoroteradecanoic acid in the solutions was varied between 0.2-1.0 mM, which corresponds to particles where less than 45% of the sites are occupied with perfluorotetradecanoate. Stearic acid chemisorbs to fill the remainder of the vacant sites. Similar diiodomethane contact angles were observed for the CM particles and the perfluorotetradecanoate functionalised particles where the concentration of perfluoroteradecanoic acid was above 0.5 mM (Figure 4a). In addition, the sliding angles of the liquid were much lower for the CM coatings compared to those that were solely functionalized with perfluorotetradecanoate in this concentration range (Figure 4b). However, similarly to particles that were solely functionalized by the fluorinated carboxylate, reducing the concentration of perfluorotetradecanoic acid to below 0.6 mM was observed to create surfaces where diiodomethane was more strongly adherent and would not roll off. This suggests that

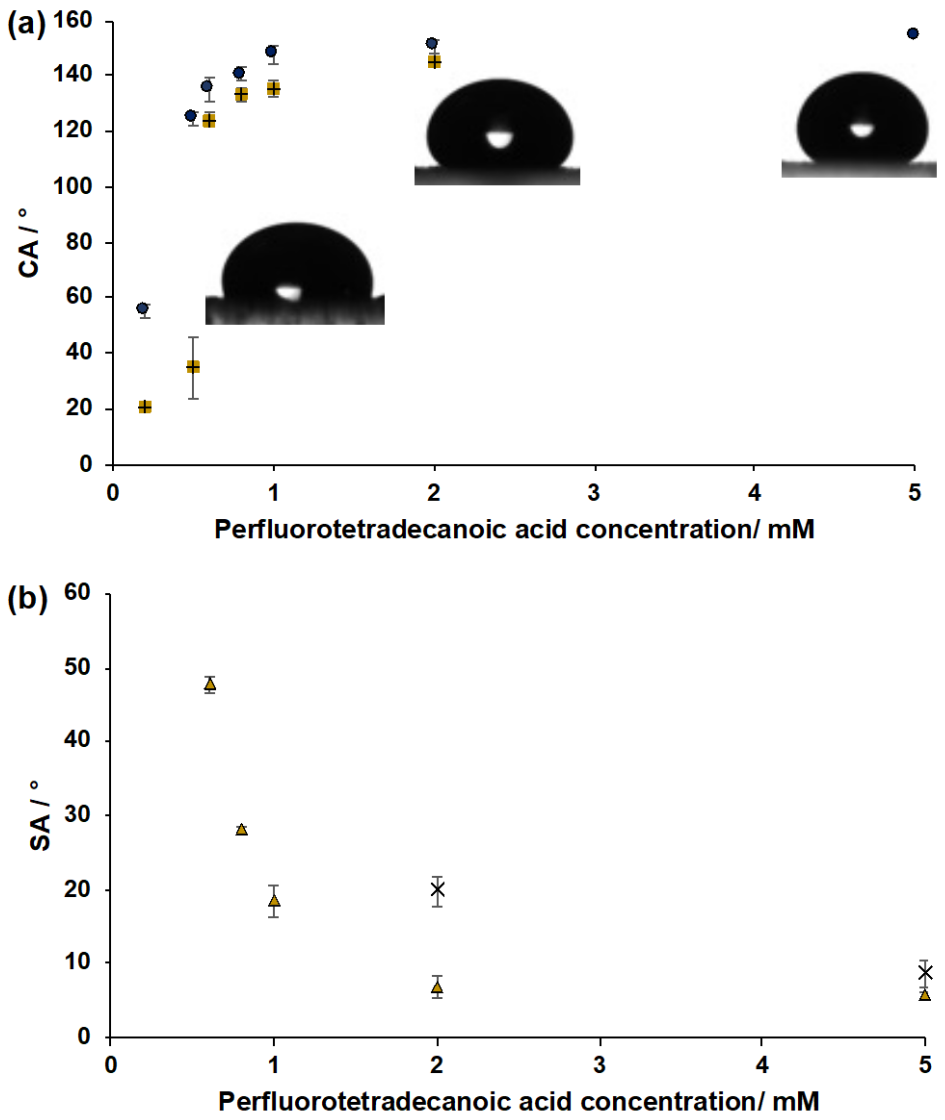

Figure 3. Water (blue circles) and CH_2I_2 (yellow plus signs) contact angles (a), and water (crosses) and CH_2I_2 (yellow triangles) sliding angles (b), of the aluminum oxide nanoparticle coatings as a function of the perfluorotetradecanoic acid concentration. Images of 4 µl diiodomethane droplets are shown in the inset of (a). The droplets are on coated surfaces functionalized by 5.0, 1.0 and 0.8 mM perfluorotetradecanoic acid (right to left).

diiodomethane rolling is at least largely governed by the coverage of the surface by the fluorinated chains. Reducing the concentration of perfluoroteradecanoic acid to below 0.5 mM in the mixed

solutions created surfaces that were more oleophobic relative to those prepared using solutions that did not contain stearic acid. For example, coatings prepared using the 0.5 mM perfluoroteradecanoic acid mixed solution showed a diiodomethane contact angle of about 107°, whereas the contact angle of coatings prepared using a 0.5 mM solution without stearic acid showed a contact angle of only 35 °. This could suggest that perfluorotetradecanoate is more evenly distributed across the particles when stearate is also present on the surface, which results in more oleophobic coatings.

Occupation of vacant sites on the particles with stearate was also observed to improve the hydrophobicity of the coatings. Particles that had been immersed in the mixed solutions showed water contact angles greater than 150° for all of the concentrations of perfluoroteradecanoic acid investigated (Figure 4a), unlike coatings solely functionalized by perfluorotetradecanoate. In addition, sliding angles for water droplets were observed for all of the mixed coatings, unlike coatings prepared using solutions containing just perfluorotetradecanoic acid. Sliding angles between 11-21° were measured for these surfaces (Figure 4b) and it was not apparent that there was a relationship between the fluorocarbon content and the water sliding angle. This indicates that adsorption of carboxylic acids bearing hydrocarbon groups onto vacant sites can robustly improve the hydrophobicity of the coatings such that they display Cassie-Baxter wetting towards water at all of the fluorocarbon concentrations.[2] Due to these wettability differences, this data indicates that it is possible to reduce fluorocarbon concentrations in omniphobic coatings through employing mixtures of carboxylic acids containing both hydrocarbon and perfluorocarbon chains. Creating coatings that would show equivalent omniphobic behavior using solely fluorocarbons would require larger amounts of perfluorotetradecanoic acid, which would increase the environmental hazards and cost associated with using this methodology.

PM coatings formed from mixtures of particles that were fully saturated with either stearate or perfluorooctadecanoate showed similar water and diiodomethane contact angles to the CM films. These physically mixed coatings showed diiodomethane contact angles between 133-141° when the mass fraction of perfluorodecanoate functionalized particles in the film exceeded 30% (Figure 5a). In this range, the diiodomethane sliding angles were observed to decrease steadily from 17 ° to 6 °. Lower diiodomethane contact angles were observed when the amount of fluorinated particles in the coating dropped below 30% (Figure 5a) and a sliding angle of approximately 45 ° was observed for the coating created using 20% perfluorotetradecanoate particles (Figure 5b), indicating the greater adhesion of the liquid to the surface. Water contact angles of greater than 150 º were observed for all of the PM coatings and sliding angles of water droplets on the surfaces were observed to increase between 5-20 ° as the fluorocarbon content was steadily lowered. This indicates that similarly to the CM coatings, coatings formed from the PM nanoparticles showed Cassie-Baxter wetting towards water for all of the fluorocarbon concentrations.

Surface free energy (SFE) measurements were performed on selected surfaces using water and diiodomethane droplets (Table 2). As anticipated, it was observed that the surfaces showed very low components of the polar component of the SFE, γ_p, indicating that they do not engage with molecules in these liquids through polar interactions, such as dipole-dipole interactions or hydrogen bonding.[29, 30] Instead, the major contribution to the total SFE is through the dispersive component, γ_d. Surfaces functionalized by fluorocarbons have been observed to show lower γ_d, than metal oxide or hydrocarbon functionalized surfaces[29, 30]. This is due to the low polarizability of the C-F bonds, which limits the extent to which they can engage with molecules through Van Der Waals interactions[5-7]. Nanoparticles that were partially saturated with perfluorotetradecanoate were observed to show the largest γ_p, which is ascribed to water molecules interacting with areas

of the unfunctionalised aluminum oxide surface. For example, coatings prepared from particles immersed in a 1.0 mM perfluorotetradecanoic acid solution showed a γ_p of 0.11 (Table 2 entry 2), which is substantially higher than the CM or PM coatings, where the surfaces are saturated by the carboxylates. It was not possible to measure the SFE of surfaces functionalized solely by stearate since these coatings were observed to be superoelophilic towards diiodomethane, which arises as a result of the dispersive interactions between the hydrocarbon chains of the surface-grafted carboxylate and diiodomethane molecules.[27, 28] Interestingly, the CM coating prepared using the same concentration of perfluorotetradecanoic acid (Table 2 entry 4) showed both lower γ_p and γ_d, which could suggest that the distribution of perfluorotetradecanoate is more homogenous when stearate is co-adsorbed onto the surface. This is because the alkyl chains of the adsorbed stearate interact strongly with diiodomethane, therefore their presence would not be expected to increase the contact angle and thus lower the SFE. Similar observations have been reported for fluorocarbon functionalized SiO_2 particles, so this assertion is not implausible.[31] By comparison, coatings formed from particles saturated with perfluorotetradecanoate showed lower SFE than the CM coating, arising from the complete occupation of surface sites with the fluorocarbon chains (Table 2 entry 1). Interestingly, it was observed that increasing the amount of perfluorotetradecanoate functionalized particles in the PM coatings past 30% was observed to create surfaces with similarly low SFE values (Table 2 entry 5), despite the coatings possessing lower fluorocarbon content than the CM coating. This result is also ascribed to the distribution of fluorinated material on the surface and could suggest that fluorinated groups become more homogenously distributed across the surface of PM films relative to CM films, which results in lower SFE and lower wettability. It has been observed that island-like growth of individual adsorbates has been shown to occur on surfaces immersed in solutions containing different types of adsorbate. Consequently, it is plausible that

the larger chemical heterogeneity of the CM films over the PM films could stem from the presence of phase-separated areas of the fluorinated and non-fluorinated carboxylates on the surface of the nanoparticles.[32]

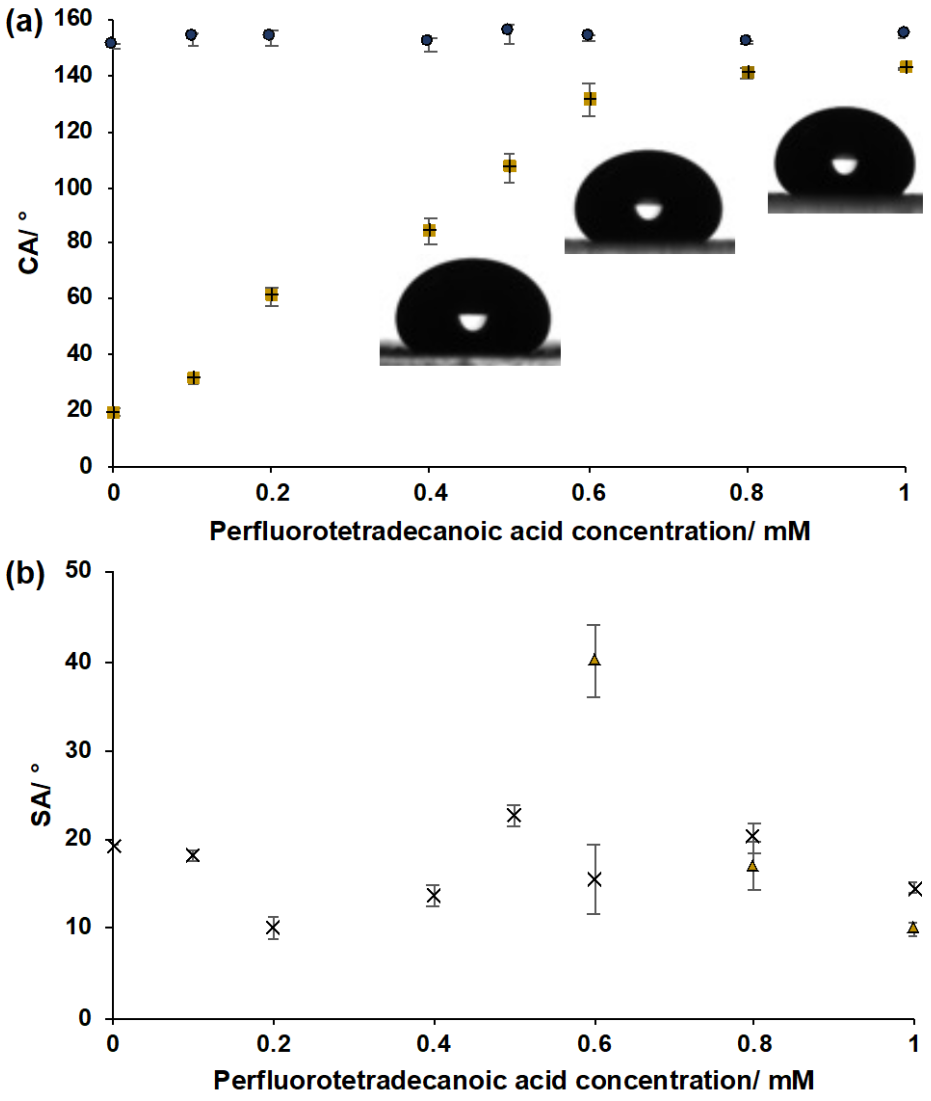

Figure 4. Water (blue circles) and CH_2I_2 contact angles (yellow plus signs) (a), water sliding angles (crosses) and CH_2I_2 sliding angles (yellow triangles) (b), of the CM coatings as a function of the perfluorotetradecanoic acid concentration. Images of 4 µL diiodomethane droplets are shown in the inset of (a). The droplets are on coated surfaces functionalized by 1.0, 0.8 and 0.5 mM perfluorotetradecanoic acid (right to left).

Dynamic wettability measurements using water droplets were also carried out on these selected surfaces to further probe their homogeneity (Table 2). It was observed that coatings formed from either the stearate or perfluorodecanoate particles displayed the lowest contact angle hysteresis (CAH) values. PM coatings, where the amounts of fluorinated particles exceeded 30%, showed similarly low CAH, in line with their low SFE (Table 2 entry 5). Coatings formed from CM particles possessing higher amounts of perfluorodecanoate were observed to show a slightly higher CAH (Table 2 entry 4). This could suggest that coatings where the fluorinated and non-fluorinated surface energy lowering compounds are not bound to the same particle are more homogeneous in terms of surface energy.[33, 34] Evaluating their wettability, employing PM as opposed to CM particles in coatings could offer the better approach for creating omniphobic coatings in terms of both environmental impact and financial cost. For example, the PM coating containing 30% perfluorodecanoate functionalised particles shows similar SFE and wettability towards water droplets as coatings formed from particles that are saturated with perfluorodecanoate. This coating also shows only slightly reduced oleophobicity relative to the CM coating prepared using a mixed solution of 1 mM perfluorotetradecanoic acid and 5 mM stearic acid, whilst possessing a lower amount of fluorocarbon. Furthermore, analysis of the monetary costs associated with fabricating these surfaces, show that both the PM and CM coatings are far cheaper to manufacture than coatings saturated using perfluorotetradecanoic acid alone (Table 2) as a result of the substantially lower amounts of adsorbed fluorocarbon. Given that the cost of stearic acid is approximately £0.06 g^{-1}, this suggests that employing either the CM or PM coatings as an alternative to a solely fluorinated coating can produce a coating with lower environmental impact and financial cost, without compromising on wettability. For example, if a company required 100 kg of carboxylic acid for use as material for coating, it would cost £ 190000 if solely perfluorotetradecanoic acid

was used, using the price listed in Table 2. Whereas, it would cost £ 61200 if the PM coating containing 30% perfluorotetradecanoic acid and 70% stearic acid was used, which amounts to a saving of approximately two thirds. Investigations into the wettability of the PM coating containing 30% of the fluorinated particles and the nanoparticle coating that was fully saturated with fluorocarbon were performed using liquids with lower surface tensions. It was observed that both coatings became significantly less oleophobic when the surface tension of the test liquid dropped below 47 mNm^{-1}. It has been shown that re-entrant surface topographies are required for fluorinated surfaces to repel liquids with surface tensions in this range.[35-40] As discussed, SEM did not show that nanoparticle coatings possessed this kind of morphology. Consequently, the drop in oleophobicity can be explained on this basis. More detail about these experiments is given in the supporting information.

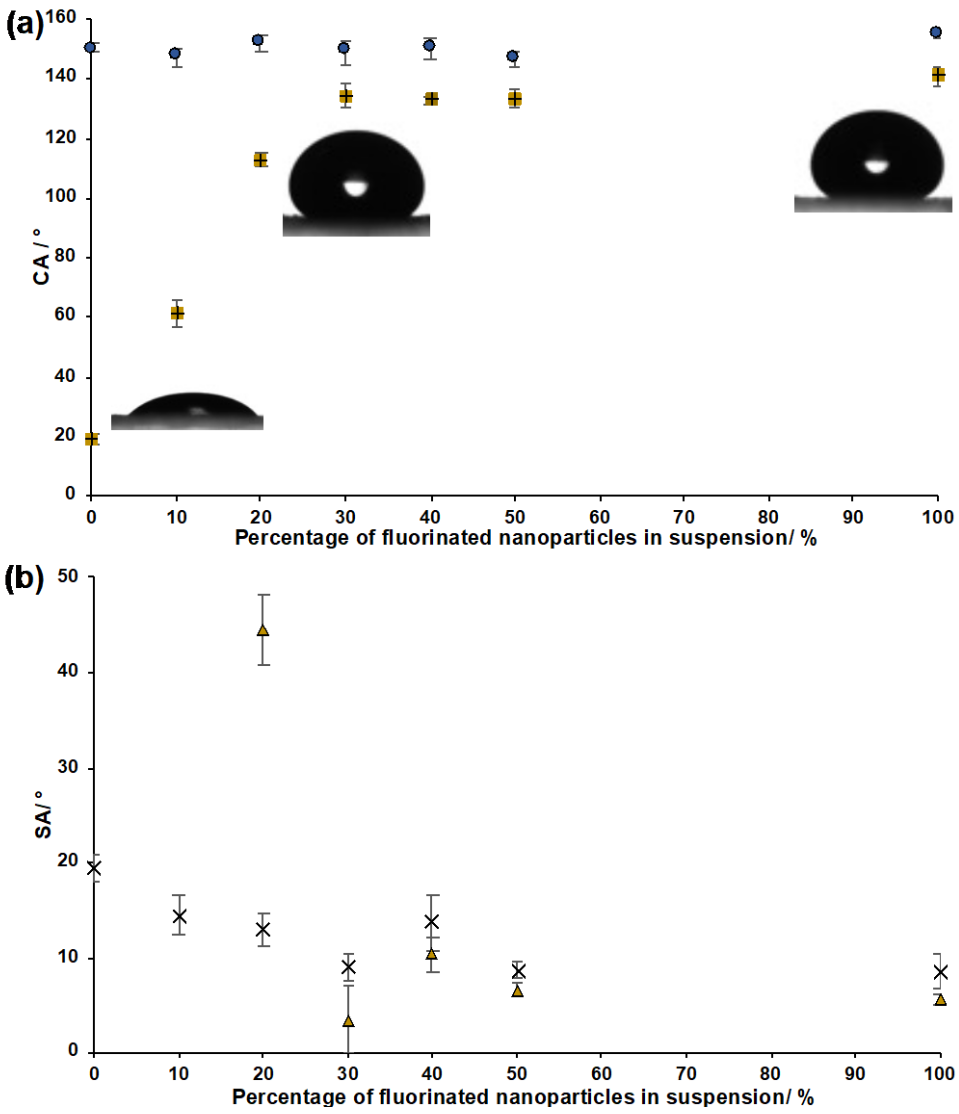

Figure 5. Water (CAs) (blue circles) and CH_2I_2 contact angles (yellow plus signs) (a), water sliding angles (crosses) and CH_2I_2 sliding angles (yellow triangles) (b), of the PM coatings as a function of the percentage of fully fluorinated particles in the spraying suspension. Images of 4 µL diiodomethane droplets are shown in the inset of (a). The droplets are on coated surfaces containing 100, 30 and 10 % perfluorotetradecanoate functionalized particles (right to left).

Table 2. Wettability data and fluorocarbon content of selected nanoparticle coatings[a].

Type of coating	% FC	WCA/ °	H_2O CAH/ °	H_2O SA/ °	CH_2I_2 SA/ °	γ_p/ mNm^{-1}	γ_d/ mNm^{-1}	Cost of FC/ £g^{-1}
100% FC	15.8	151 ± 1	10	17 ± 3	6 ± 1	0.00 ± 0.01	0.43 ± 0.07	1.90
45% FC	7.1	148 ± 4	34	–	18 ± 2	0.11 ± 0.05	1.18 ± 0.24	0.85
100% HC	0.0	150 ± 1	12	20 ± 1	–	–	–	0.00
(1:5 mM HC:FC) CM coating	7.1	154 ± 1	19	15 ± 3	10 ± 1	0.00 ± 0.01	0.61 ± 0.04	0.85
30% FC PM coating	4.7	149 ± 3	11	9 ± 1	17 ± 4	0.00 ± 0.01	0.35 ± 0.04	0.56

[a]Fluorocarbon (FC) costs of perfluorotetradecanoic acid were taken from the Merck Life Sciences website. The cost quoted is the amount of FC adsorbed onto the nanoparticles determined using TGA.

Fouling resistance towards viscoelastic solids. To date, the majority of research that has been carried out studying omniphobic coatings has involved investigating their repellency towards liquids. Although much work has been done exploring what effects liquid viscosity has on wetting behaviour and adhesion, coatings that show low adhesion to mixtures containing solids have been far less studied.[35-37] Employment of these coatings on materials such as glass, or plastics for food packaging, where contact with viscoelastic solids occurs, could be useful for preventing fouling of these surfaces. For food packaging this might result due to contact of the surface with viscous and sticky foods, such as sauces and dairy products, and through contact with biological mixtures, such as animal faeces, for coatings that are exposed to outside environments. With this is in mind, we have studied the sliding properties of mixtures of synthetic faeces, employing the recipe used Wang *et al.*, on the PM and CM coatings.[41]

In our experiments we placed the mixture onto our samples and measured the angle at which the material would slide off the surfaces under gravity, in a manner similar to that used in sliding angle measurements for liquids. It was observed that the sliding angles of the mixture on the cleaned glass ranged between 56-60° (Figure 6a). Coatings formed from the stearate functionalised particles showed similar sliding angles to this, which could arise as a result of the dispersive interactions between oil and hydrocarbons in the mixture and stearate chains. In addition, residue was observed on the surfaces following the experiments (Figure 6c and e, and Figure S15a). By comparison, the sliding angles of mixtures on coatings fully saturated with perfluorotetradecanoate showed lower sliding angles, between 40-47°, which is ascribed to the low value of the dispersive component of the surface energy. In line with this, less oily residue was observed on the samples (Figure 6 (e) and (f)) because of their lower surface energy and thus lower adhesion between the mixture and the surfaces. PM coatings containing 40% or more perfluorodecanoate functionalized

particles also displayed similar behavior to this and showed tilt angles ranging between 40-53 º and showed similarly low amounts of oily residue to the coating that was fully saturated with perfluotetrardecanoate (SI Figure 13b). Interestingly, coatings formed from CM particles possessing larger fluorocarbon contents than the PM coatings were not observed to substantially reduce the sliding angle of the mixture on the surfaces. As discussed previously, these coatings show increased water CAH, relative to PM coatings with similar fluorocarbon contents. Given that the viscoelastic mixture is largely comprised of water, this could suggest that the surfaces' larger wettability towards water is responsible for the larger sliding angle. Studies into the durability of the nanoparticle coatings are presented in the supporting information.

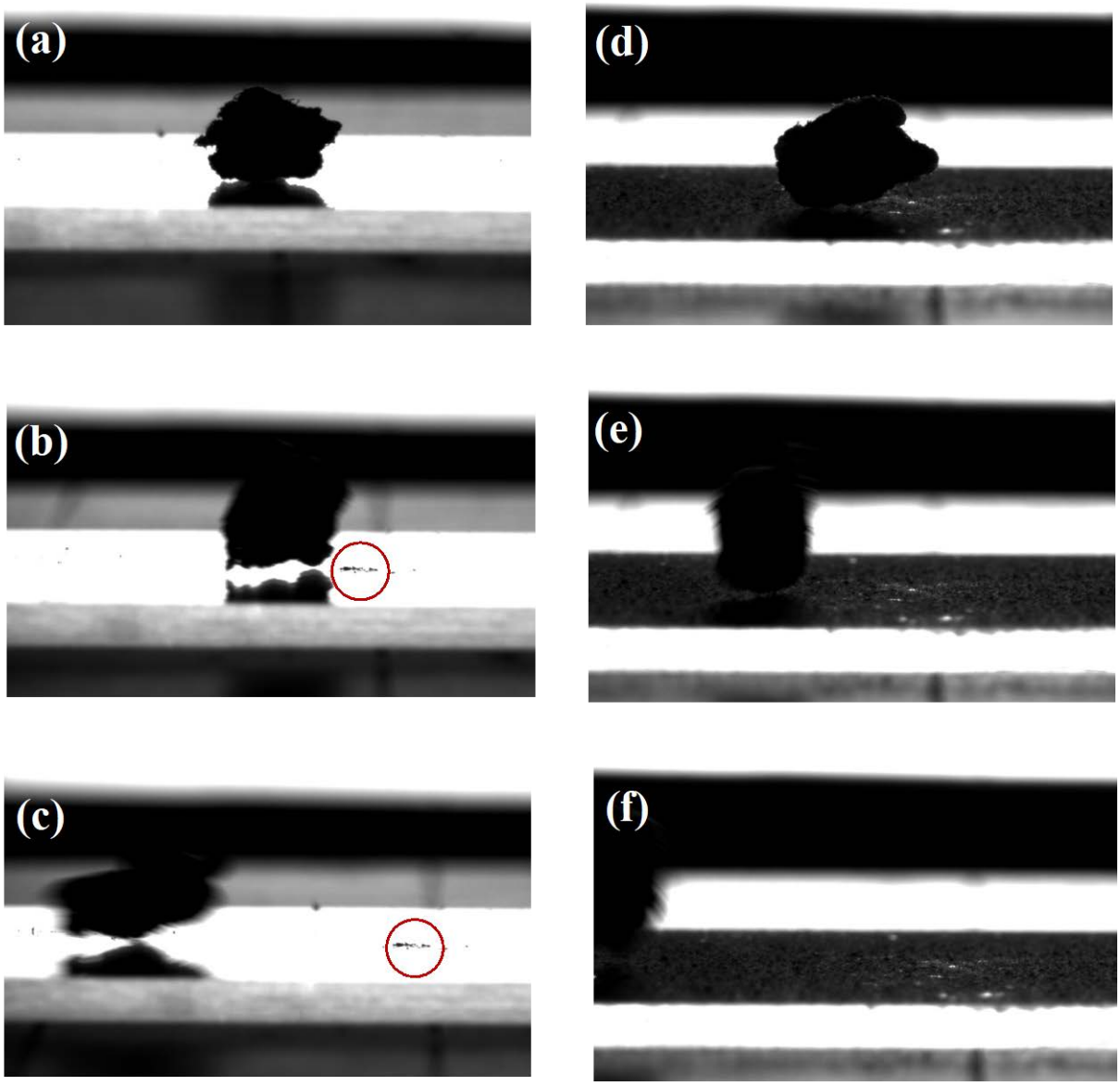

Figure 6. Images of the synthetic faeces mixture on the cleaned glass (a, b and c) and a nanoparticle coating on glass that is fully saturated with perfluorodecanoate (d, e and f). Residue is marked by red circles.

Conclusion

This work indicates that it is possible to substantially lower the fluorocarbon content present in coatings formed from functionalized nanoparticles, without significantly reducing their wettability towards water or diiodomethane. Previous work in the field of omniphobic coatings has studied altering the fluorocarbon chain length to lower the environmental impact.[19, 20] However, to our knowledge, developing a greener approach using nanoparticle films formed from hybrid particles functionalized by compounds possessing both hydro- and fluorocarbon groups has not yet been reported. Our research indicates that it is possible to reduce the fluorocarbon content in the coatings by as much as 70%, without substantially compromising properties such as CAs, sliding angles, or CAH. We have observed that this is possible either through applying coatings where the hydro- and fluorocarbon groups are present on different particles, physical mixtures (PM), or where these groups are co-adsorbed on the same particles, CM particles. SFE and CAH measurements indicate that it is possible to create omniphobic coatings with slightly lower fluorocarbon contents through using physical as opposed to chemical mixtures of the particles, which could suggest that the fluorocarbon chains are more homogeneously distributed across the surface of these coatings. This is line with previous studies, where island-like growth of adsorbates has been observed on surfaces when they have been immersed in solutions containing chemically dissimilar adsorbate molecules.[32] Consequently, physical mixtures of hydro- and fluorocarbon functionalized particles may be better candidates more creating more environmentally friendly omniphobic coatings, relative to coatings where these groups are co-adsorbed onto the same particles. Films formed from the CM particles would be suitable for applications where a lower degree of omniphobicity is required since the data shows that they possess greater efficacy than films functionalized solely by the same amount of fluorocarbon. In addition, they may also be more attractive surfaces from a

synthesis perspective since manufacturers would only need fabricate one type of nanoparticle as opposed to two, which could make the process more economically viable. Differences in wettability of the PM coatings were observed when the amounts of fluorinated particles in the coatings was lowered to 30%, where they were observed to show lower contact angles towards low surface tension liquids relative to analogous coatings fully saturated with fluorocarbon. This indicates that the fluorocarbon content in PM of hydrocarbon: fluorocarbon particles needs to be tuned depending on the fouling liquids that they are expected to come into contact with. In addition to this behavior, we have also observed that the PM coatings show similar repellency to viscoelastic solids, like synthetic faeces, to analogous coatings that are saturated by fluorocarbons, which provides further evidence of their functionality as robust anti-fouling coatings.

MATERIALS AND METHODS

Materials. Aluminum oxide nanopowder (13 nm mean particle size, average 100 m^2g^{-1} specific surface area), stearic acid, perfluorotetradecanoic acid, isopropanol, ethanol, cellulose, calcium chloride, sodium chloride and potassium chloride were purchased from Merck Life Sciences. The carboxylic acids were used without any further purification. Glass microscope slides were obtained from Fisher Scientific and VWR Chemicals. Miso paste and peanut oil were bought from local shops. Psylum husks were purchased from Wholefoods.

Functionalization of the aluminum oxide nanoparticles. Adsorption of perfluorotetradecanoic acid onto the nanoparticles was achieved through immersing 100 mg of the nanopowder in isopropanolic solutions containing concentrations of the carboxylic acid ranging between 0.2-15 mM. The resulting mixtures were stirred for twenty-four hours at room temperature and then centrifuged at 5000 rpm for one hour in order to collect the nanoparticles.

The supernatant was then removed. Following this, the nanoparticles were re-dispersed in isopropanol and centrifuged at 5000 rpm for one hour in order to remove unreacted carboxylic acids. The supernatant was discarded following this. This process was then repeated one further time using ethanol to disperse the particles. The functionalized material was then dried at 100 ºC for at least three hours. Similarly, the adsorption of stearic acid onto the nanoparticles was studied through immersing 100 mg of the nanopowder into 100 mL isopropanolic solutions containing concentrations of stearic acid ranging between 1-15 mM and stirring the mixtures for twenty-four hours at room temperature. The purification procedure was the same as what is described for the perfluorotetradecanoic acid functionalized particles. Co-functionalization of the particles with both stearic and perfluorotetradecanoic acid was carried out through immersing the nanopowder in 100 ml isopropanolic solutions containing both of these carboxylic acids. The concentration of stearic acid was fixed at 5 mM whilst the concentration of perfluorotetradecanoic acid was varied between 0.1-1 mM. Both carboxylic acids were observed to readily dissolve in this solvent in this concentration range when subjected to ultrasonication for several minutes. The purification procedure was the same as what is described for the other two types of particles. Experiments where one carboxylate was exchanged for another was carried out through stirring 100 mg of the functionalised particles in 100 mL isopropanolic solutions containing 10 mM of either stearic or perfluorotetradecanoic acid.

Film deposition. Nanoparticle films were spray coated onto glass microscope slides using an artist's spray gun and hydrocarbon airbrush propellant from 2 wt.% isopropanolic suspensions. The microscope slides were washed with acetone before film deposition. Suspensions used to spray the physically mixed nanoparticle films were stirred for 1-2 hours ahead of use. All other suspensions were stirred between 5-10 minutes prior to spray coating. Three layers of the

suspensions were applied to the slides during spray coating and the samples dried under ambient conditions.

Preparation of the synthetic faeces. Synthetic faeces was prepared through first physically mixing yeast (6 wt.%), cellulose (3 wt.%), sodium chloride (0.5 wt.%), potassium chloride (0.5 wt.%), calcium chloride (0.25 wt.%) and psylum husk (4 wt.%) with a spatula. Peanut oil (3 wt.%) was then added and mixed thoroughly, followed by Miso paste (2 wt.%). Water (81.25 wt.%) was then mixed in by hand. The solid was covered and left to stand for one hour at ambient conditions before use.

Characterization. Wettability studies were carried out using a Krüss DSA25 Expert Drop Shape Analyzer using Krüss Advance software (1.6.2.0). Static contact angles (CAs) were performed using 4 µL droplets of the test liquids at three different locations on the surfaces. Surface free energy (SFE) calculations were performed by placing three 4 µL droplets of diiodomethane and deionized water at different positions on the surfaces. SFE values were calculated using the OWRK model. Sliding angle measurements were carried out through tilting the samples from 0-90 º using the instrument's tilting table at a rate of approximately 1 $^{o}s^{-1}$. Sliding angles were defined as the angle at which the liquid droplet had left the camera's field of view. Experiments were also conducted in the same manner using the synthetic faeces mixture. Sliding angles were taken as the angle at which the solid left the camera's field of view. One levelled spatula of the mixture was placed on the surfaces during the tests. Advancing and receding contact angle measurements were performed through dosing a 4 µL water droplet with water at a rate of 0.5 $\mu L.s^{-1}$ until its volume reached 34 µL. Water was then removed from the droplet at a rate of 0.5 $\mu L.s^{-1}$ until its volume returned to 4 µL. Advancing and receding water contact angles were measured as the volume of the droplet changed during the process. Infrared spectroscopy was performed using a Thermo

scientific i510 spectrometer with attached ATR. Four scans were performed on each material with a resolution of 4 cm^{-1}. Thermogravimetric analysis (TGA) was carried out using a TA Instrument SDT Q600. The particulates were loaded into alumina crucibles and heated to 650 ºC from ambient conditions, under continuous air flow. The heating rate used was 20 °C.min^{-1} and the materials were heated isothermally for a further ten minutes when the temperature had reached 650 ºC. Scanning electron microscopy (SEM) was performed using a Hitachi S4800 scanning electron microscope. Imaging was performed using a 1.0 kV accelerating voltage. Atomic Force Microscopy (AFM) was carried out using a JPK Nanowizard in tapping mode. Surface roughness measurements were performed on three different 20×20 μm^2 areas of the surfaces. Parameters discussed are the average of the three measurements, whilst the variations are described by the standard deviations.

ASSOCIATED CONTENT

Supporting Information. The following files are available free of charge. Word document containing TGA curves of the fluorinated and HC nanoparticles, IR spectra of the stearate and perfluorooctadecanoate functionalized nanoparticles, SEM and AFM images of the coatings and surface roughness analysis. Images of the test liquids on selected surfaces. Further discussion about carboxylate adsorption onto the particles, the durability of the films, and wettability of the films towards other liquids are also contained in this file.

AUTHOR INFORMATION

Corresponding Author

Shirin Alexander - *Energy Safety Research Institute (ESRI), Swansea University Bay Campus, Fabian Way, Swansea SA1 8EN, United Kingdom.* 0000-0002-4404-0026

Authors

Donald Hill - *Energy Safety Research Institute (ESRI), Swansea University Bay Campus, Fabian Way, Swansea SA1 8EN, United Kingdom.* 0000-0002-3457-5895

Henry Apsey - *Energy Safety Research Institute (ESRI), Swansea University Bay Campus, Fabian Way, Swansea SA1 8EN, United Kingdom.* 0000-0001-6095-7646

Andrew R. Barron - *[1]Energy Safety Research Institute (ESRI), Swansea University Bay Campus, Fabian Way, Swansea SA1 8EN, United Kingdom. [2]Arizona Institutes for Resilience (AIR), University of Arizona, Tucson, Arizona 85721, USA. [3]Department of Chemistry and Department of Materials Science and Nanoengineering, Rice University, Houston, Texas 77005, USA. [4]Faculty of Engineering, Universiti Teknologi Brunei, BE1410, Brunei Darussalam.* 0000-0002-2018-8288

Author Contributions

The manuscript was written through contributions of all authors. All authors have given approval to the final version of the manuscript.

Funding Sources

The Welsh Government Sêr Cymru Programme provided financial support through the Sêr Cymru Chair for Low Carbon Energy and Environment, the Reducing Industrial Carbon Emissions

(RICE) operations funded by the Welsh European Funding Office (WEFO) through the Welsh Government (ARB), We gratefully acknowledge Salts Healthcare Ltd for providing financial support for this project (DH, HA). EPSRC DTP is also acknowledged for PhD studentship (HA).

Notes

The authors declare no competing financial interest.

ACKNOWLEDGMENTS

We would like to acknowledge the Centre of Nanohealth (CNH) and the SPECIFIC project for use of their imaging equipment when characterizing the surfaces.

REFERENCES

1. Yong, J.; Chen, F.; Yang, Q.; Huo, J.; Hou, X. Superoleophobic surfaces, *Chem. Soc. Rev.* **2017**, *46*, 4168-4217.

2. Ragesh, P.; Ganesh, V. A.; Nair, S. V.; Sreekumaran Nair, A. A review on 'self-cleaning and multifunctional materials, *J. Mater. Chem. A* **2014**, *2*, 14773-14797.

3. Wang, Y.; Gong, X. Special oleophobic and hydrophilic surfaces: approaches, mechanisms, and applications, *J. Mater. Chem. A* **2017**, *5*, 3759-3773.

4. Liu, X.; Liang, Y.; Zhou, F.; Liu, W. Extreme wettability and tunable adhesion: biomimicking beyond nature? *Soft Matter* **2012**, *8*, 2070-2086.

5. Zhang, D.; Huang, C.; Luo, W.; Wu, Y.; Long, Z. Study of oleophobic modification of fiber material surface and its performance, *Fibers and Polymers* **2019**, *20*, 1145-1154.

6. Brown, P. S.; Bhushan, B. Durable, superoleophobic polymer–nanoparticle composite surfaces with re-entrant geometry via solvent-induced phase transformation, *Sci. Rep.* **2016**, *6*, 21048.

7. Brown, P. S.; Bhushan, B. Designing bioinspired superoleophobic surfaces, *APL Mater.* **2016**, *4*, 015703.

8. Leng, B.; Shao, Z.; de With, G.; Ming, W. Superoleophobic cotton textiles, *Langmuir* **2009**, *25*, 2456–2460.

9. Aslanidou, D.; Karapanagiotis, I. Superhydrophobic, superoleophobic and antimicrobial coatings for the protection of silk textiles, *Coatings*, **2018**, *8*, 101-114.

10. Aslanidoua, D.; Karapanagiotisb, I.; Panayiotoua, C. Superhydrophobic, superoleophobic coatings for the protection of silk textiles, *Prog. Org. Coat.,* **2016**, *97*, 44-52.

11. Al-Shatty, W.; Lord, A. M.; Alexander, S.; Barron, A. R. Tunable surface properties of aluminum oxide nanoparticles from highly hydrophobic to highly hydrophilic, *ACS Omega*, **2017**, *2*, 2507-2514.

12. Ma, Z.; Wu, Y.; Xu, R.; Li, Z.; Liu, Y.; Liu, J.; Cai, M.; Bu, W.; Zhou, F. Robust Hybrid Omniphobic Surface for Stain Resistance, *ACS Appl. Mater. Interfaces*, 2021, *13*, 14562−14568.

13. Senthilkumar, K.; Ohi, E.; Sajwan, K.; Takasuga, T.; Kannan, K. Perfluorinated compounds in river water, river sediment, market fish, and wildlife samples from Japan, *Bull. Environ. Contam. Toxicol.* **2007**, *79*, 427–431.

14. Lau, C.; Butenhoff, J. L.; Rogers, J. M. The developmental toxicity of perfluoroalkyl acids and their derivatives, *Toxicol. Appl. Pharmacol.* **2004**, *198*, 231–241.

15. Prevedouros, K.; Cousins, I. T.; Buck, R. C.; Kozeniowski, S. H. Sources, fate and transport of perfluorocarboxylates, *Environ. Sci. Tech.* **2006**, *40*, 32-44.

16. Kennedy Jr., G. L.; Butenhoff, J. L.; Olsen, G. W.; O'Connor, J. C.; Seacat, A. M.; Perkins, R. G.; Biegel, L. B.; Murphy, S. R.; Farrar, D. G. The toxicology of perfluorooctanoate, *Crit. Rev. Toxicol.* **2004**, *34*, 351-384.

17. Gilliland, F. D.; Mandel, J. S. Mortality among employees of a perfluorooctanoic acid production plant, *J. Occup. Med.* **1993**, *35*, 950-954.

18. Milman, O. Covid: chemicals found in everyday products could hinder vaccine, *The Guardian*, 17th November 2020.

19. Zhang, Q.; Wang, Q.; Jiang, J.; Zhan, X.; Chen, F. Microphase structure, crystallization behavior, and wettability properties of novel fluorinated copolymers poly(perfluoroalkyl acrylate-co-stearyl acrylate) containing short perfluorohexyl chains, *Langmuir* **2015**, *31*, 4752-4760.

20. Jiang, J.; Zhang, G.; Wang, Q.; Zhang, Q.; Zhan, X.; Chen, F. Novel fluorinated polymers containing short perfluorobutyl side chains and their super wetting performance on diverse substrates, *ACS Appl. Mater. Interfaces* **2016**, *8*, 10513-10523.

21. Chen, H.; Zhu, S. S. Controlling water-mediated interactions by designing self-assembled monolayer coatings, *Sci. Rep.* **2021**, *11*, 8459-8467.

22. Rajiv, S.; Jerobin J.; Saranya, V.; Nainawat, M.; Sharma, A.; Makwana P.; Gayathri, C.; Bharath, L.; Singh, M.; Kumar, M.; Mukherjee, A.; Chandrasekaran N. Comparative cytotoxicity and genotoxicity of cobalt (II, III) oxide, iron (III) oxide, silicon dioxide, and aluminum oxide nanoparticles on human lymphocytes in vitro, *Hum Exp Toxicol.* **2016**, *35*, 170-183.

23. Alexander, S.; Eastoe, J.; Lord, A. M.; Guittard, F.; Barron, A. R. Branched hydrocarbon low surface energy materials for superhydrophobic nanoparticle derived surfaces, *ACS Appl. Mater. Interfaces* **2016**, *8*, 660-666.

24. Hill, D.; Attia, H.; Barron, A. R.; Alexander, S. Size and morphology dependent surface wetting based on hydrocarbon functionalized nanoparticles, *J. Colloid Interface Sci.* **2019**, *543*, 328-334.

25. Hill, D.; Barron, A. R.; Alexander, S. Controlling the wettability of plastic by thermally embedding coated aluminium oxide nanoparticles into the surface, *J. Colloid Interface Sci.* **2020**, *567*, 45–53.

26. Hill, D.; Holliman, P. J.; McGettrick, J.; Searle, J.; Appelman, M.; Chatterjee, P.; Watson, T. M.; Worsley, D. A. Studies of inherent lubricity coatings for low surface roughness galvanized steel for automotive applications, *Lubri. Sci.* **2017**, *29*, 317-333.

27. Jańczuk, B.; Wójcik, W.; Zdziennicka, A. Determination of the components of the surface tension of some liquids from interfacial liquid-liquid tension measurements, *J. Colloid Interface Sci.* **1993**, *157*, 384-393.

28. Wang, L.; McCarthy, T. J. Covalently attached liquids: instant omniphobic surfaces with unprecedented repellency, *Angew. Chem.* **2016**, *128*, 244-248.

29. Colorado Jr, R.; Lee, T. R. Wettabilities of self-assembled monolayers on gold generated from progressively fluorinated alkanethiols, *Langmuir* **2003**, *19*, 3288-3296.

30. Colorado Jr, R.; Lee, T. R. Physical organic probes of interfacial wettability reveal the importance of surface dipole effects, *J. Phys. Org. Chem.* **2000**, *13*, 796-807.

31. Cai, Y.; Li, J.; Yi, L.; Yan, X. Li, J. Fabricating superhydrophobic and oleophobic surface with silica nanoparticles modified by silanes and environment-friendly fluorinated chemicals, *Appl. Surf. Sci*. **2018**, *450*, 102-111.

32. Marquez, M. D.; Zenasni, O.; Jamison, A. C.; Lee, T. R. Homogeneously Mixed Monolayers: The Emergence of Compositionally Conflicted Interfaces *Langmuir* **2017**, 33, 8839-8855.

33. Drelich, J.; Miller, J. D. The effect of solid surface heterogeneity and roughness on the contact angle/drop (bubble) size relationship. *J. Colloid Interf. Sci.* **1994**, *164*, 252–259.

34. Drelich, J.; Miller, J. D.; Good, R. J. The effect of drop (bubble) size on advancing and receding contact angles for heterogeneous and rough solid surfaces as observed with sessile-drop and captive-bubble techniques. *J. Colloid Interf. Sci* **1996**, *179*, 37–50.

35. Zhu, Q.; Li, B.; Li, S.; Luo, G.; Zheng, B.; Zhang, J. Durable superamphiphobic coatings with high static and dynamic repellency towards liquids with low surface tension and high viscosity, *J. Colloid Interf. Sci*. **2020**, *578*, 262-272.

36. Li, X.; Wang, D.; Tan, Y.; Yang, J.; Deng, X. Designing transparent micro/nano re-entrant-coordinated superamphiphobic surfaces with ultralow solid/liquid adhesion, *ACS Appl. Mater. Interfaces* **2019**, *11*, 29458-29465.

37. Zhang, H.; Ji, X.; Liu, L.; Ren, J.; Tao, F.; Qiao, C. Versatile, mechanochemically robust, sprayed superomniphobic coating enabling low surface tension and high viscous organic liquid bouncing, *J. Chem. Eng.* **2020**, *402*, 126160.

38. Tuteja, A.; Choi, W.; Ma, M.; Mabry, J. M.; Mazzella, S. A.; Rutledge, G. C.; McKinley, G. H.; Cohen, R. E. Designing superoleophobic surfaces, *Science* **2007**, 318, 1618-1622.

39. Chen, L.; Guo, Z.; Liu, W. Outmatching superhydrophobicity: bio-inspired re-entrant curvature for mighty superamphiphobicity in air, *J. Mater. Chem. A* **2017**, *5*, 14480-14507.

40. Kota, A. K.; Tuteja, A.; Mabry, J. M. Superoleophobic Surfaces: design criteria and recent studies, *Surf. Innov.* **2013**, *1*, 71-83.

41. Wang, J.; Wang, L.; Sun, N.; Tierney, R.; Li, H.; Corsetti, M.; Williams, L.; Wong, P. K.; Wong, T. Viscoelastic solid-repellent coatings for extreme water saving and global sanitation. *Nat. Sustain.* **2019**, *2*, 1097-1105.

Table of Contents Graphic